Journal of Catalysis 319 (2014) 61–70

Contents lists available at ScienceDirect

Journal of Catalysis

journal homepage: www.elsevier.com/locate/jcat

On the process for furfural and HMF oxidative esterification over Au/ZrO_2

Federica Menegazzo [a], Tania Fantinel [a], Michela Signoretto [a,*], Francesco Pinna [a], Maela Manzoli [b]

[a] Department of Molecular Sciences and Nanosystems, Ca' Foscari University Venice and INSTM-RU Ve, Dorsoduro 2137, 30123 Venezia, Italy
[b] Department of Chemistry & NIS Interdepartmental Centre, University of Turin, Via P. Giuria 7, 10125 Turin, Italy

ARTICLE INFO

Article history:
Received 9 June 2014
Revised 21 July 2014
Accepted 23 July 2014

Keywords:
Gold catalyst
Au
Zirconia
Furfural
5-HMF
Oxidation
Esterification
Biomass

ABSTRACT

The process for the oxidative esterification of furfural and HMF on Au/ZrO_2 catalyst has been deeply investigated. Many variables, such as reaction time, temperature, pressure, and nature of the oxidant, have been optimised. For both processes, a considerable effect of the reaction temperature has been evidenced in the range here investigated (60–140 °C). As regards furfural, oxygen pressure can be lowered from 6 to 1 bar without significant changes in the catalytic performances. Molecular oxygen can be replaced by the more economic air, still at very low relative pressure (0.5 bar). In the case of HMF, oxygen pressure can be lowered from 6 to 1 bar without significant changes in the catalytic performances. Data on the reaction mechanism have been also verified by FTIR spectroscopy measurements taken in opportune experimental conditions in order to mimic reaction conditions.

1. Introduction

Bio-renewable fuels and chemicals are becoming increasingly important as we continue to deplete our finite petroleum resources. A great effort is being expended in industry and academia to develop processes to produce chemical intermediates from bio-based sources that can replace petrochemicals in existing products [1].

Currently, there is an intensive research on the use of lignocellulosic raw material as a biomass source for producing chemicals and fuels. Plant biomass consists mainly of carbohydrates, lignin, protein and fats. Out of an estimated 170 billion metric tons of biomass produced every year, roughly 75% are in the form of carbohydrates which makes biomass carbohydrates the most abundant renewable resource [2]. This makes carbohydrates the centre of attention when looking for new and greener feed stocks to replace petroleum for producing commodity. It is therefore important to continue to develop processes that can economically convert lignocelluloses into chemicals. 2-Furaldehyde (furfural) is a C5 compound and it is industrially manufactured for a long time through hydrolysis of pentose which comes from agricultural raw materials (see upper part of Scheme 1).

Actually furfural has many different uses, but additional transformations are highly desired [3]. Furfural can be transformed in alkyl furoates, which find applications as flavour and fragrance components in the fine chemical industry.

On the other hand, 5-hydroxymethyl furfural (HMF) is considered an important and renewable platform chemical in the bio-based renaissance as a dehydration product of hexoses. HMF plays an important role, because it can be obtained not only from fructose, sucrose and inulin but also, more recently, from glucose *via* isomerisation to fructose, as well as directly from cellulose [4]. HMF is an important versatile intermediate that can be further transformed into a wide variety of high performance and high value-added chemicals [5]. In particular, HMF can be oxidised to 2,5-furandicarboxylic acid (FDCA), that is a monomer for the synthesis of polymers alternative to those obtained from terephthalic acid. For instance, polyethylene terephthalate (PET) is a polymer commonly made into fibres, resins, films, etc., and it is one of the highest tonnage and fastest growing plastic materials [6]. Actually, PET is mainly manufactured by the purified terephthalic acid whose process, jointly developed by Scientific Design and Amoco [7,8], is based on the liquid-phase oxidation of p-xylene. However, the harmful effects of bioaccumulation in living organisms of both phthalates and derived polymers have been known for a long time. Besides being obtained from a bio-derived, renewable raw material, the polymer got from FDCA (PEF), is more easily degradable

* Corresponding author.
E-mail address: miky@unive.it (M. Signoretto).

http://dx.doi.org/10.1016/j.jcat.2014.07.017
0021-9517/

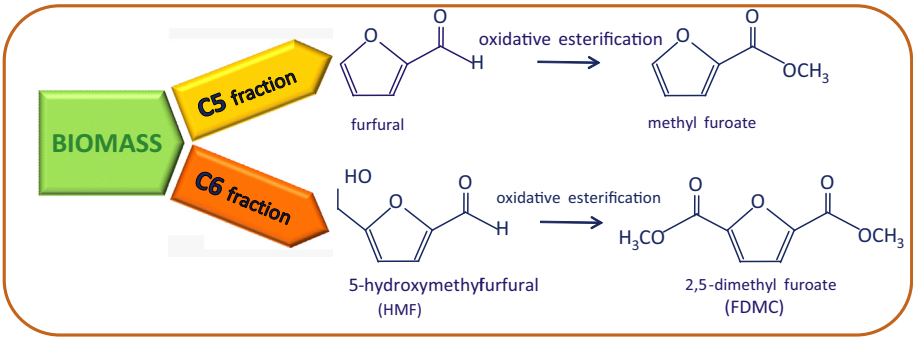

Scheme 1.

and above all, it does not present problems of bioaccumulation. A study commissioned by the U.S. Department of Energy identified FDCA as one of the 12 potentially useful building blocks for value-added chemicals from biomass [9]. Unfortunately, FDCA is practically insoluble in most of the solvents industrially used. HMF can be transformed by oxidative esterification into the corresponding furan-2,5-dimethylcarboxylate (FDMC) as reported in Scheme 1, lower part. The latter molecule is easily purified by low-temperature sublimation to give high purity FDMC, which is readily soluble in the most common solvents and therefore it could be even more suitable than FDCA as monomer for the replacement of terephthalic acid in plastics [10,11].

PEF has some better physical properties than PET, such as higher gas impermeability (10 times compared to oxygen, 4 times compared to carbon dioxide and 2 times compared to water) and higher glass transition temperature (for the PEF = 86 °C while for the PET = 74 °C). Finally, PEF production could be made in the same facilities used for PET [12]. As a demonstration of the importance of this polymer, the "Coca Cola" company has recently signed a trade agreement with "Avantium" for the development and production on industrial scale of this polymer in order to replace PET bottles with PEF bottles [12].

Christensen et al. [10] have firstly demonstrated that good yields in the oxidative esterification of furfural and HMF can be obtained with a commercial Au/TiO_2 catalyst provided by the World Gold Council in the presence of a base (8% CH_3ONa). However, the use of the base makes the process less green and less advantageous from an economic point of view [11]. Subsequently, Corma et al. [11] tested these reactions over gold-based catalysts on different supports, but without using the base. However, only one catalyst dispersed on ceria nanoparticles showed satisfactory performances for HMF oxidative esterification, while Au/C, Au/CeO_2, Au/TiO_2, Au/Fe_2O_3 samples require reaction times ranging from 24 to 72 h to get still very low yields. Very recently, we investigated gold catalysts supported on zirconia [13,14], ceria and titania [15] for a base-free esterification of furfural. In particular, we identified the physicochemical properties that render gold supported on zirconia an active, selective and recyclable catalyst [14,15].

In the last years, some reviews [16–18] have been published on the selective oxidation of furan derivates meaning that a great attention has been paid to these reactions. From literature studies, it is possible to affirm that the choice of gold nanoparticles is advantageous for the oxidative esterification reactions. However, it would be advantageous to optimise the operating conditions in order to make the process environmentally friendly and industrially feasible. Basing on these premises, the goals of the present work are:

(1) to prove the effective mechanism of the oxidative esterification performed over gold supported on zirconia under our reaction conditions;

(2) to find the best process conditions, in terms of pressure, temperature, nature of the oxidising agent and reaction time, in order to yield a greener, safer, economic and sustainable process.

2. Experimental

2.1. Catalyst preparation

$Zr(OH)_4$ was prepared by precipitation from $ZrOCl_2{\cdot}8H_2O$ at constant pH = 8.6 and then aged for 20 h at 90 °C. The hydroxide was sulphated with $(NH_4)_2SO_4$ (Merck) by incipient wetness impregnation in order to obtain a 2 wt% amount of sulphates on the final support. Then, sulphated zirconium hydroxides (SZ2) were calcined in air (30 ml/min STP) at 650 °C for 3 h.

2 wt% of gold was added by deposition–precipitation (DP) at pH = 8.6: The oxide was suspended in an aqueous solution of $HAuCl_4{\cdot}3H_2O$ for 3 h and the pH was controlled by the addition of NaOH (0.5 M). After filtration, the sample was dried at 35 °C overnight and finally calcined in air for 1 h at 400 °C. 2 wt% of SO_4^{2-} was found on the calcined support before DP. On the contrary, no sulphates are present in the final AuZ catalyst anymore. This is due to the detachment of sulphate groups during the DP at pH = 8.6 [19]. The Au/TiO_2 catalyst provided by the World Gold Council (WGC) was also studied as a reference. Table 1 summarises the characterisation data of the examined gold catalysts.

2.2. Methods

The sulphate content was determined by ion chromatography (IC). Sulphate concentration was calculated as the average of two independent analyses, each including two chromatographic determinations.

The gold amount was determined by atomic adsorption spectroscopy after microwave destruction of the samples (100 mg).

CO pulse chemisorption measurements were taken at −116 °C in a lab-made equipment. Before the analysis, the following pretreatment was applied: The sample (200 mg) was reduced in a H_2 flow (40 ml/min) at 150 °C for 60 min, cooled in H_2 to room temperature, purged in He flow and finally hydrated at room temperature. The hydration treatment was performed by contacting the sample with a He flow (10 ml/min) saturated with a proper amount of water. The sample was then cooled in He flow to the temperature chosen for CO chemisorption (−116 °C) [20].

FTIR measurements of adsorbed molecules were carried out on the samples in self-supporting pellets introduced in a cell allowing thermal treatments in controlled atmospheres and spectrum scanning at controlled temperatures (from −196 °C to 25 °C). The FTIR spectra were taken on a PerkinElmer 1700 spectrometer (equipped with a cryogenic MCT detector). From each spectrum, the spectrum of the sample before the inlet of the molecule was subtracted. The

Table 1
Characterization data of the gold catalysts.

Sample	Label	Preparation method	Au loading (wt%)	mol_{CO}/mol_{Au}	d_m (nm)
Au/ZrO_2	AuZ	DP	1.22	0.045	2.3 ± 0.5
Au/TiO_2	AuT_{WGC}	DP	1.51	0.033	3.8 ± 0.7

spectra were normalised with respect to the weight of the pellet and to the effective gold content reported in Table 1.

The activation pretreatment to which the AuZ sample was undergone, consisted in two steps: (i) oxidation (outgassing up to 150 °C, then in O_2 from 150 °C up to 180 °C and further cooling to room temperature (RT) in O_2 atmosphere) in order to clean the surface from carbonate species and water, due to the exposition to air and (ii) reduction in H_2 at 150 °C, outgassing from 150 °C to RT. In the case of $AuT_{WGC,}$ the following procedure was adopted: (i) oxidation (outgassing up to 200 °C, then in O_2 from 200 °C up to 400 °C and final cooling to RT in O_2) and (ii) reduction in H_2 at 250 °C and further cooling in H_2 to RT under outgassing.

2.3. Catalytic activity measurement

Furfural or HMF oxidative esterifications with oxygen or air were investigated without $NaCH_3O$ addition, using a mechanical stirred autoclave fitted with an external jacket [14]. Catalyst (100 mg), substrate (300 μl furfural or 200 mg HMF, Sigma-Aldrich 99%) and *n*-octane (150 μl), used as internal standard, were added to the solvent (150 ml of methanol or ethanol). The reactor was charged with the oxidant (0.5–6 bar of relative pressure), stirred at 1000 rpm and heated at a proper temperature in the range 60–140 °C. The progress of the reaction was determined typically after 90 min (if not specified otherwise) by gas chromatographic analysis of the converted mixture (capillary column HP-5, FID detector). Preliminary experiments showed that the system works in a strictly kinetic regime [14].

3. Results and discussion

3.1. Investigation on the reaction mechanism

3.1.1. Furfural oxidative esterification

A possible oxidation–esterification pathway has been previously supposed by Corma and co-workers for their gold on nanoparticulated ceria [11]. According to this investigation, furfural is firstly transformed in the hemiacetal intermediate, which is not detectable by a gas chromatographic analysis. Then, the reaction can follow two different routes: The former involves the direct oxidation of the hemiacetal into the methyl-2-furoate (furoate), whereas in the latter, the hemiacetal is firstly transformed in the corresponding 2-furaldehyde-dimethyl-acetal (acetal). The acetal can lead to the furoate.

In order to clarify and to validate the oxidation–esterification pathway under our reaction conditions, we have carried out some different tests on the AuZ catalytic system, as reported in Scheme 2, where R = —H:

(1) A first catalytic test was performed without the catalyst, i.e. the autoclave was charged with furfural, *n*-octane, methanol and 6 bar of O_2. After 3 h of reaction at 120 °C, no trace of furoate, acetal or other products was found, meaning that the catalyst is crucial for the reaction.
(2) In order to completely rule out the furoate formation *via* furoic acid, we have performed a catalytic test with the AuZ catalyst in the typical reaction conditions but using furoic acid as substrate instead of furfural. In this case no furoate was produced.

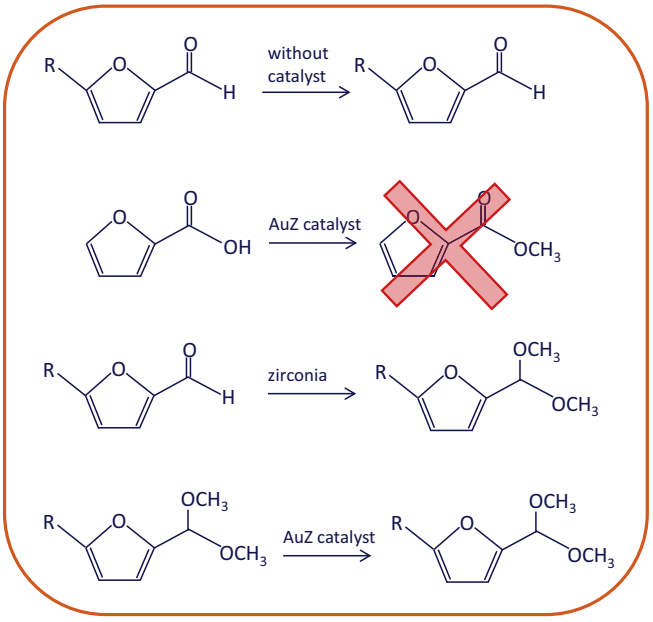

Scheme 2. Investigation on the mechanism for the oxidative esterification of furfural (R = —H) and HMF (R = —CH_2—OH).

(3) In another investigation, the autoclave was charged in the typical reaction conditions, except for the catalyst: bare zirconia (both plain zirconia and sulphated zirconia) was loaded, instead of AuZ. In this case, a complete (100%) furfural conversion was found, however acetal was the only reaction product. It can be inferred that the Lewis acidity displayed by zirconia [21,22] is able to get a full transformation of furfural into the corresponding acetal. On the other hand, this experiment demonstrates that the presence of the gold active phase is essential for the formation of the desired furoate.
(4) Another test was performed in order to check if the acetal molecule can be transformed in the furoate over the gold-based catalyst under reaction conditions. After the reaction at point (3) carried out in the presence of the bare support, the solution was filtered and separated from solid zirconia. Then the solution, containing acetal in methanol, was charged in the autoclave together with the AuZ catalyst. Only acetal was found after the catalytic test. Therefore, furfural can be converted into acetal in the presence of the bare support; however, due to its stability, acetal cannot be transformed into the desired furoate.

The catalytic experiments showed that in the presence of AuZ, the reaction proceeds through direct selective oxidation of furfural to the desired furoate. Moreover, the AuZ catalyst guarantees an almost complete selectivity to methyl-2-furoate. On the contrary, in the presence of the bare support, the reaction leads to the formation of the acetal molecule, which is stable under reaction conditions, and it cannot be further transformed. Gold active phase is crucial for producing the desired furoate and it can be hypothesised that oxygen activation takes place on highly dispersed gold

exposed at the surface of this catalyst [13–15]. From these results, we can conclude that under our conditions, the reaction with AuZ involves the direct furfural esterification to obtain the methyl-2-furoate.

In Fig. 1 (section a), the furfural conversion and selectivity to methylfuroate for AuZ and AuT_{WGC} catalysts are shown. The AuZ sample shows very good catalytic performances; in particular, after 90 min, both conversion and selectivity are almost complete. On the contrary, for the AuT_{WGC} sample, catalytic performances are noticeably lower (at 90 min conversion 63%, selectivity 62%).

In order to achieve a more deep understanding on the reaction mechanism, the interaction with the reactant (furfural) and the product (methylfuroate) with both AuZ and AuT_{WGC} catalysts was investigated by FTIR spectroscopy. FTIR spectra collected on the AuZ catalyst after interaction with the furfural molecule as well as after interaction with methyl-2-furoate are reported in Fig. 2, sections a and b, respectively. The spectra of free furfural and methylfuroate liquid molecules are shown in the same figure (grey curves in section a and section b, respectively).

The comparison among the spectra of the adsorbed molecules with those related to the free molecules (black bold curves vs. grey curves) pointed out that both furfural and methylfuroate interact mainly through their carbonylic group with the surface of the catalyst. This behaviour is confirmed by looking at the spectra of the adsorbed molecules in the C=O stretching region (1800–1650 cm^{-1} range): Here, the spectra appear more perturbed if compared to the finger print region (1650–1000 cm^{-1}). The variety of observed bands is an indication that different interactions involving several geometries of the molecules and possibly different kinds of sites exposed at the surface of AuZ. Moreover, looking at the intensity of the bands in the C=O stretching region, furfural seems to interact more strongly with the surface of the catalyst than what the methylfuroate does.

The same experiments have been performed on AuT_{WGC}, and analogous observations can be done also in such case. For the sake of comparison, the spectra collected on the AuT_{WGC} catalyst after the inlet of methylfuroate are reported in Fig. S1.

CO adsorption at RT was performed on as prepared AuZ (grey curve) as well as on the sample after interaction with furfural (bold curve, section a) and methylfuroate (bold curve, section b). The results are reported in sections a and b of Fig. 3. CO adsorption on as prepared AuZ produced a band at 2162 cm^{-1}, due to CO on Zr^{4+} sites of the support [23], and a quite symmetric band at

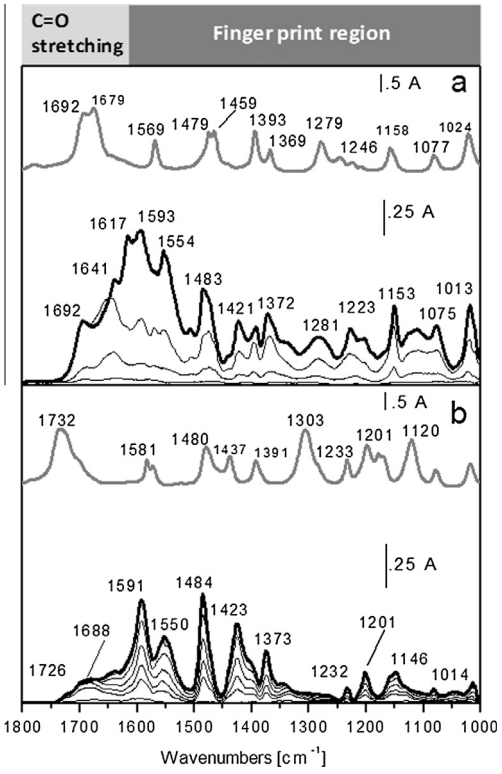

Fig. 2. FTIR absorbance spectra collected on AuZ after inlet of 1 mbar and subsequent outgassing of furfural (section a, black curves) and of methylfuroate (section b, black curves) at RT. FTIR absorbance spectra of liquid furfural and liquid 2-methylfuroate are reported as references (grey curves).

2100 cm^{-1}, that by decreasing the CO pressure decreases in intensity without shifting its position, due to CO on highly dispersed gold [19] (grey curves in sections a and b). The comparison between the bold curves and the grey ones indicates that after interaction with furfural (section a) and methylfuroate (section b), the band at 2162 cm^{-1} totally disappeared, whereas the band at 2100 cm^{-1} is unchanged as for position and intensity (according to the dashed line positioned at 2100 cm^{-1}, as a guide to the eye). This experiment highlighted that both furfural and methylfuroate exclusively interact with the catalyst, leaving free the gold

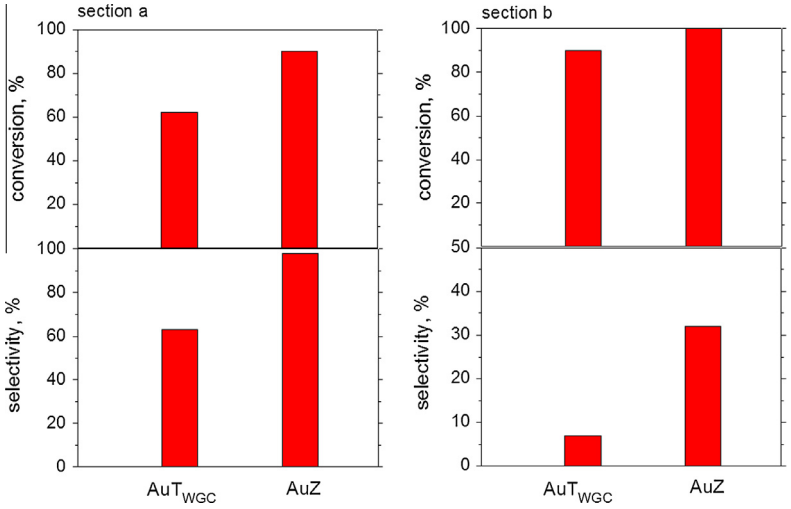

Fig. 1. Catalytic performances in the furfural (section a) and HMF (section b) oxidative esterification reactions on the AuZ and AuT_{WGC} catalysts. (*Reaction conditions:* section a: 120 °C, 6 bar O_2, after 90 min and section b: 130 °C, 3 bar O_2, after 5 h.)

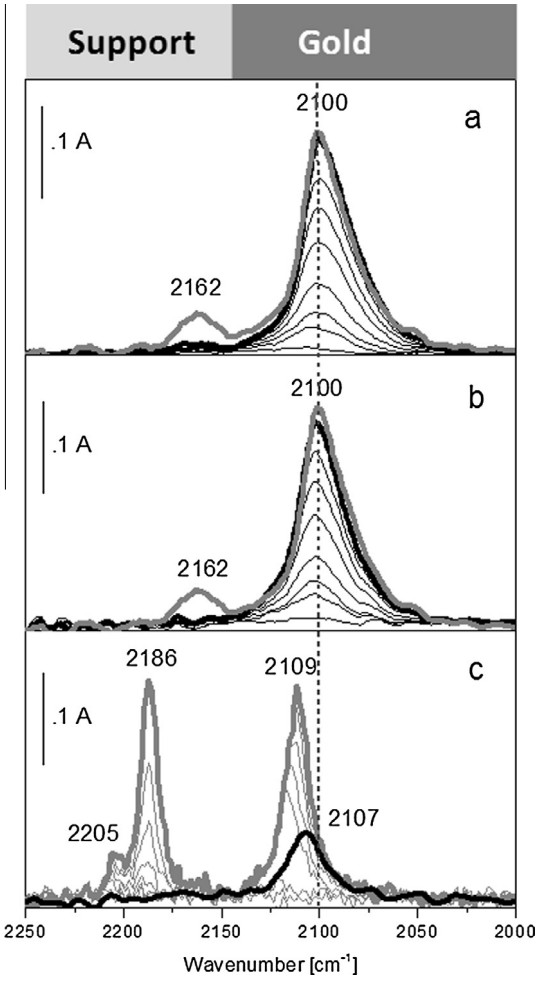

Fig. 3. FTIR absorbance spectra collected after inlet of 20 mbar CO on as prepared AuZ (grey curves, sections a and b) and AuT_{WGC} (grey curves, section c) and on the samples after interaction with furfural (bold curve, section a) and methylfuroate (bold curve, sections b and c) and subsequent outgassing (fine curves).

uncoordinated sites able to adsorb CO. A totally different behaviour has been observed when performing the same experiment on AuT_{WGC} (section c of Fig. 3). Beside the depletion of the bands at 2205 and 2186 cm^{-1}, due to CO on Ti^{4+} sites [24], the methylfuroate molecule is also interacting with the uncoordinated gold sites. The different behaviour towards CO adsorption can be explained firstly by taking into account the different affinity of each support towards these molecules (the intensity of the bands in Fig. S1 is higher than that of those reported in Fig. 3, section b). Moreover, the different gold particle sizes observed for the two catalysts (see Table 1) can possibly play a role, too. Before contacting with methylfuroate, the band at 2109 cm^{-1} blueshifts in position upon decrease in the CO pressure (grey curves) indicating that the Au sites are not isolated. Moreover, this band displays also a different shape, i.e. it is asymmetric towards the lower frequencies. These features are typically observed when CO is adsorbed on gold nanoparticles at room temperature [25]. Therefore, the Au dispersion is lower on AuT_{WGC} than on AuZ. Upon contacting with methylfuroate, the band at 2109 cm^{-1} is decreased in intensity, shifted at 2107 cm^{-1} and changed in shape: In fact, it is broader and quite symmetric. These features can be interpreted by assuming that the methylfuroate molecule is able to adsorb on the uncoordinated gold sites exposed at the surface of the nanoparticles (according to the decrease in intensity of the band after contact with the molecule) as well as it is able to induce a modification of these sites, according to the changes in shape and position upon interaction. It can be proposed that the strength of the CO bond is decreased due to the perturbation induced by methylfuroate in terms of steric hindrance.

The different affinity towards furfural and methylfuroate as well as the different gold dispersion can be at the origin of the contrasting catalytic performances displayed in the furfural and HMF oxidative esterification reactions by AuZ and AuT_{WGC} catalysts.

Finally, such kind of measurements allowed us also to distinguish the bands related to the adsorbed reactant from those due to the formed product. In particular, as will be illustrated later on (Fig. 4) and basing on the data presented in Figs. 2 and S1, we have specifically referred to the absence/presence of a band at 1715–20 cm^{-1}, due to C=O stretching mode of adsorbed methylfuroate.

FTIR measurements on the furfural oxidative esterification reaction were also taken and the results are reported in Fig. 4. Both AuT_{WGC} (section a) and AuZ (section b) catalysts were contacted with the reaction mixture (oxygen, 15 mbar, methanol, 1 mbar and furfural, 1 mbar) at RT, and then, the temperature was increased at 120 °C, that is the temperature at which the maximum conversion and selectivity are observed (as shown in Fig. 11).

Different bands associated with the C—O and C—H stretching vibration modes of methoxy species are produced on AuT_{WGC} (section a) and on AuZ (section b) upon methanol interaction at RT (black curves). Moreover, they have also different relative intensities on the two samples. On AuT_{WGC}, the bands related to methoxy species increase in intensity when the temperature is increased at 120 °C (red curve), indicating further methanol dissociation on the catalyst surface. On the contrary, on AuZ, the temperature enhancement from RT to 120 °C causes a strong decrease in intensity of the band at 1157 cm^{-1}, due to one specific kind of methoxy

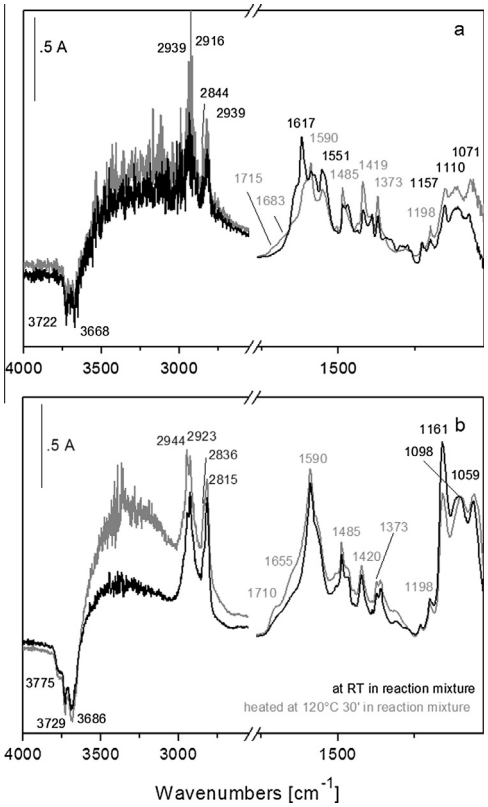

Fig. 4. FTIR absorbance spectra collected on AuT_{WGC} (section a) and AuZ (section b) catalysts contacted with the reaction mixture (oxygen, 15 mbar, methanol, 1 mbar and furfural, 1 mbar) at RT (black curve) and at 120 °C (grey curve).

species, simultaneously to the increase in the bands related to methylfuroate, while the others do not change significantly in intensity. The observed behaviour can be an indication that methoxy species, possibly bridged on Zr^{4+} and Au sites at the perimeter of the metal nanoparticles close to the support [23,24,26,27], are directly involved in the furfural esterification reaction. Moreover, the intensity of the band related to this species is more abundant on AuZ than on AuT_{WGC} after interaction with methanol at room temperature (data not shown) in agreement with the observed catalytic trend.

Focusing on the 1750–1200 cm^{-1} spectroscopic range, bands related to adsorbed methyl-2-furoate, whose frequencies are reported in grey in the figure, are formed on AuT_{WGC} (grey curve in Fig. 3, section a) only upon increasing the temperature at 120 °C. On the contrary, these bands are observed already at RT on AuZ (black curve in section b) and further increase in intensity when the temperature reached 120 °C (grey curve).

The spectroscopic findings confirm that the formation of the product occurs without the formation of any adsorbed intermediate species and confirm that in the presence of AuZ, the reaction proceeds through direct selective oxidation of furfural to the desired furoate, as previously discussed (see Scheme 2). Moreover, AuZ is able to catalyse the furfural esterification already at RT, giving an almost complete selectivity to methyl-2-furoate. On the other hand, AuT_{WGC} is less active, corroborating the catalytic results reported in Fig. 1 (section a). Indeed, no reaction takes place at RT and it is necessary to heat at 120 °C to observe some reactivity.

After reaction, both catalysts were submitted to simple outgassing of the reaction mixture at RT followed by CO adsorption at the same temperature. The results are reported in Fig. 5.

After reaction, a band at 2083 cm^{-1} due to CO on gold sites [19] is produced upon CO adsorption at RT on AuZ (grey curve). The adsorption of CO on the same sample before reaction (dashed grey curve) experiments reveals that a fraction of the Au sites present on AuZ remains available after reaction. Moreover, this band is modified after reaction, but not upon interaction with furfural and methylfuroate, possibly due to the temperature (the reaction has been carried out at 120 °C, whilst both furfural and methylfuroate adsorption have been performed at RT) as well as to the presence of oxygen in the reaction mixture. In fact, the highly dispersed gold species react with O_2 producing atomic oxygen species, which can activate methanol [13,14,19]. Upon furfural and methylfuroate contacting, we did not find spectroscopic evidences of the participation to the adsorption by the uncoordinated gold sites; therefore, the band is unchanged upon interaction with these molecules. On the contrary, no bands are present on AuT_{WGC} (black curve). This feature could be related to the high and stable in time selectivity for the AuZ sample. This is a confirmation of previous studies on Au/ZrO_2 stability in the furfural oxidative esterification [14].

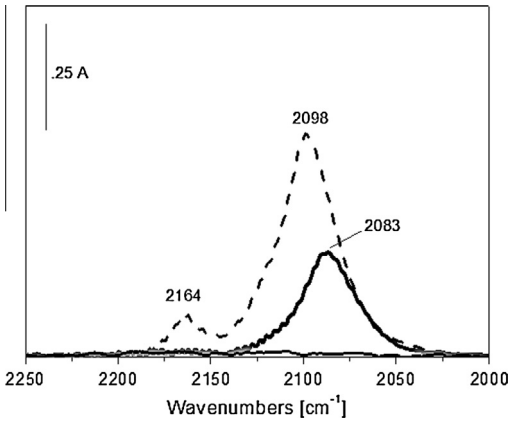

Fig. 5. FTIR absorbance spectra of 20 mbar CO adsorbed at RT on AuZ (grey curve) and AuT_{WGC} (black curve) outgassed at RT after reaction. The spectrum of CO adsorbed on the AuZ catalyst before reaction is also reported for comparison (dashed grey curve).

3.1.2. HMF oxidative esterification

Similarly, we investigated the mechanism for the reaction of HMF under our reaction conditions as well. A possible oxidation–esterification pathway has been previously supposed by Corma and co-workers for gold on nanoparticulated ceria [11]. In principle, the reaction can follow two different pathways (Scheme 3).

Catalytic tests, analogous to those performed in the case of furfural, were carried out in order to elucidate the HMF oxidation–esterification pathway under our reaction conditions and in the presence of the AuZ catalyst. We obtained the results illustrated in Scheme 1, having R = —CH_2—OH). In the presence of AuZ, the reaction follows the direct way of the oxidation from HMF into the desired FDMC (way 1), involving oxygen activation on the gold clusters. On the contrary, the reaction goes completely through the second way and leads to the acetal formation when performed in the presence of the bare support (way 2). Due to acetal stability under reaction conditions, it cannot be further transformed.

In Fig. 1 (section b), the HMF conversion and selectivity to FDMC for AuZ and AuT_{WGC} catalysts are shown. Again, the AuZ sample shows much better catalytic performances than AuT_{WGC} reference sample. However, the gap between the two catalysts is much higher than for the reaction with furfural. In fact, the presence of the ring substituent in the HMF substrate makes more difficult the reaction, decreasing the oxidation rate [11].

3.2. Oxidative esterification of furfural and HMF: optimisation of reaction conditions

3.2.1. Reaction time

First of all, the effect of the reaction time on the oxidative esterification of furfural over the AuZ catalyst was investigated. We performed different catalytic tests by varying only the time of reaction (Fig. 6).

For all catalytic tests, selectivity is very high (almost 100%) and it is constant for the time range that was investigated. These data indicate that the transformation of furfural into the corresponding furoate happens without any side reactions on the AuZ catalyst. On the contrary, as expected, the conversion increases with the reaction time. In particular, conversion rises until the maximum after 3 h of reaction.

As reported in Fig. 6, the conversion reaches 90% after 90 min of reaction. It is therefore more convenient to perform catalytic tests at 90 min of reaction. For a batch process, the halving of reaction time is fundamental: Small plants can be exploited to the maximum, allowing more cycles. After this screening, the reaction time was fixed at 90 min for all subsequent tests of furfural oxidative esterification.

A screening on the reaction times for the oxidative esterification of HMF with the AuZ catalyst is reported Fig. 7, where the concentrations of the reagent, the intermediate, and the product are shown. It can be seen that the HMF is completely converted after 3 h. The formed monoester alcohol is the intermediate of the reaction and its concentration increases up to reach a maximum at about 3 h of reaction, whereas the FDMC is produced linearly with time.

3.2.2. Effect of the pressure and of the nature of the oxidant

The research work was then addressed to the investigation of the effect of the oxygen pressure on the furfural esterificative

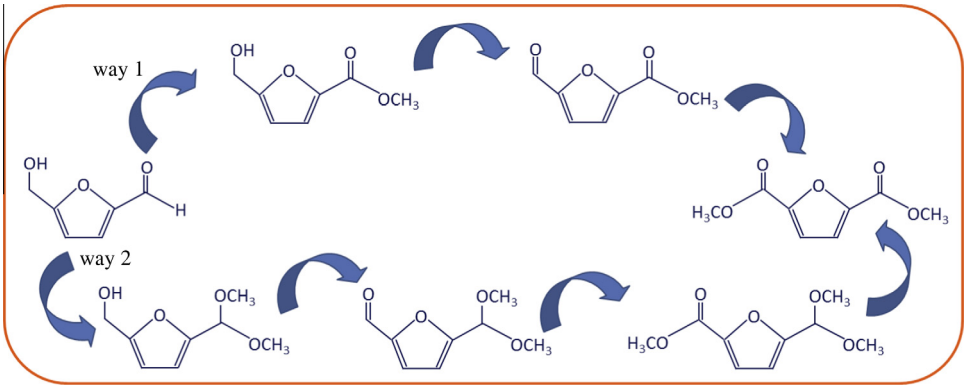

Scheme 3. Reaction pathways for HMF oxidative esterification.

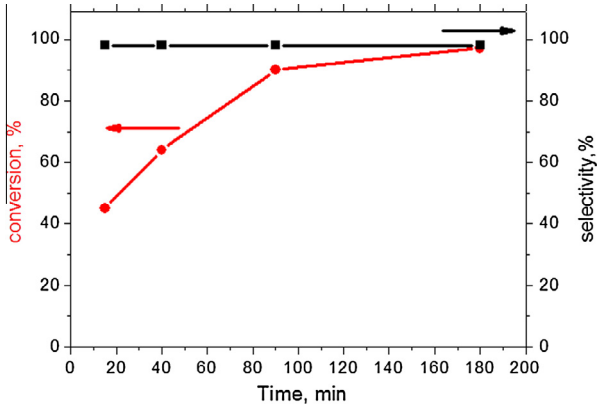

Fig. 6. Furfural oxidative esterification on the AuZ catalyst: effect of the reaction time (autoclave charged with 6 bar of O_2 – reaction at 120 °C).

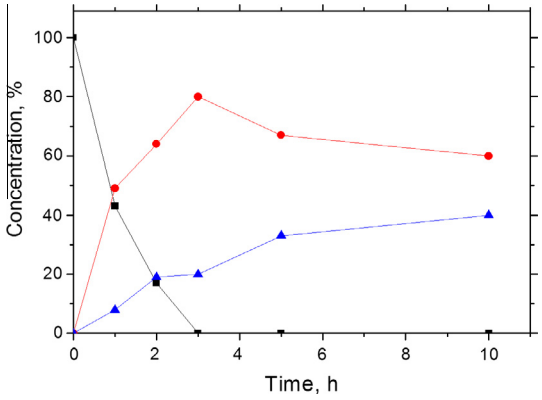

Fig. 7. HMF oxidative esterification on AuZ catalyst: effect of reaction time on the amount of reagent (■), intermediate (●) and product (▲). Autoclave charged with 3 bar of O_2 – reaction at 130 °C).

oxidation. Such effect was evaluated starting from 6 bar O_2 and dropping to lower values until 1 bar O_2 (relative pressure). As reported in Fig. 8 (section a, full bars), the pressure effect on the conversion of furfural to methyl-2-furoate is almost negligible and, despite of the pressure lowering, it is possible to obtain always high conversions.

Selectivity is constant at almost 100% and it is not affected by pressure changes. The obtained results are quite relevant, since we are able to work at very low pressures, therefore reducing the consumption of oxidant and making more harmless the experimental setup. Moreover, looking at possible application of the process on an industrial scale, the low operating pressure would lead to a decrease in costs related to plant design. Looking for further optimisation of the process conditions, the next step consisted in replacing oxygen with air in order to study the effect of the composition of the oxidant.

The graph in Fig. 8 (section a, lines bars) shows the conversions obtained using air as oxidant, by gradually lowering the pressure to a value of 0.5 bar. The conversions are very high and comparable to that in pure oxygen. The pressure appears to have no effect on the conversion up to 0.5 bar of charged air. Selectivity, as expected, is constant at almost 100% and it is not affected neither by the change from oxygen into air, nor by the reduced pressure. We decided to study the reaction in air, but at autogenous pressure. The use of atmospheric air would result into a further economic advantage. Unfortunately, in such conditions, furfural conversion is lowered: 52% instead of 70% for the reaction performed at 100 °C, even if selectivity is constant at almost 100%.

FTIR experiments were performed by contacting the AuZ catalysts with different reaction mixtures at RT and at 120 °C. The mixtures differ only by the order in which each reactant was adsorbed. The results are reported in Fig. 9.

The furfural oxidative reaction takes place when the order followed for the inlets is: oxygen, then methanol, and furfural, as demonstrated by the band at 1715 cm^{-1}, due to C=O stretching of adsorbed methylfuroate (grey curve of section a). On the contrary, if the order is: furfural, then oxygen and finally methanol, the reaction does not occur and the surface of the catalyst is covered by furfural molecules (grey curve of section b). The spectroscopic results indicate that in reaction conditions (120 °C), oxygen is fundamental to keep the active surface sites free, in particular the gold sites, where oxygen can be dissociated [13,28,29]. As a consequence, the amount of oxygen is a crucial point and the amount present in the autoclave at autogenous pressure is not stoichiometrically sufficient, in agreement with the results reported in Fig. 8.

Therefore, it is necessary to charge the autoclave with an air relative pressure, even if very low. Oxygen was completely replaced with a relative low pressure of air (0.5 bar) enabling to greatly improve the process and to maintain at the same time high conversion and selectivity. In addition, the replacement of oxygen by air allowed great advantages in terms of safety of the plant. In fact, such relative air pressure allowed to work outside the explosion limits [30], therefore largely excluding risks for operators as well as costs related to the plant management, that would be crucial for future applications.

We performed some catalytic tests applying the same reaction conditions optimised for the production of methyl-2-furoate, whilst using ethanol as both reagent and solvent. In fact, due to

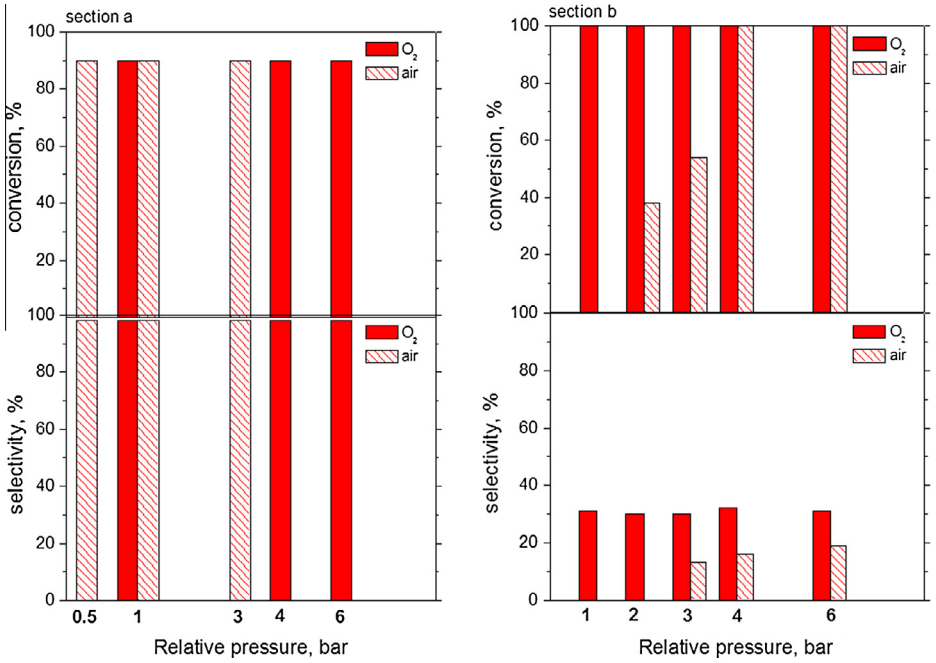

Fig. 8. Effect of the pressure on furfural (section a, 120 °C, after 90 min) and HMF (section b, 130 °C, after 5 h) oxidative esterification reactions on the AuZ catalyst.

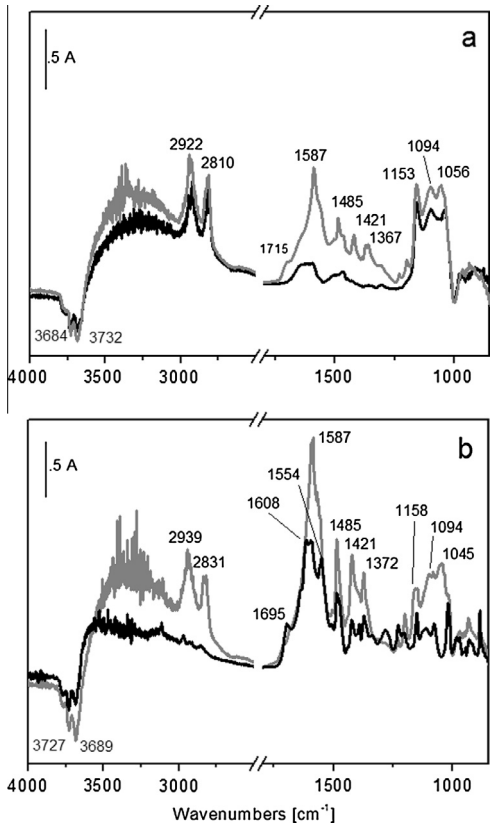

Fig. 9. FTIR absorbance spectra collected on the AuZ catalyst contacted with oxygen (15 mbar), methanol (1 mbar) and furfural (1 mbar), (section a) and furfural (1 mbar), oxygen (15 mbar) and methanol (1 mbar), (section b) at RT (black curves) and at 120 °C (grey curves).

its balsamic, burnt, and fruity floral taste, ethyl-2-furoate is used as flavouring agent, too. The results are given in Fig. 10.

Similar to what observed for HMF oxidative esterification [11], the catalytic performances are worse when ethanol is charged instead of methanol. In particular, conversion is not affected by oxygen relative pressure, which can be lowered from 3 to 1 bar, but it is in any case lower than the conversion in methanol. On the contrary, conversions in tests performed in air are noticeably lower than those obtained in tests performed in oxygen. Moreover, selectivity is around 75%, due to the formation of large amounts of ethyl-acetal and acetaldehyde.

As regards HMF oxidative oxidation, a first screening using air as oxidant was performed. Using as reaction conditions 130 °C and 5 h, the air pressure was increased from 2 up to 6 bar (relative pressure). Looking at the results shown in Fig. 8 (section b), a strong effect of air pressure on the conversion is evident. For low air pressures (2 and 3 bar), conversion is incomplete and it barely exceeds 50%. On the contrary, charging the autoclave with 4 or 6 bar of air a total conversion can be obtained. Pressure greatly influences selectivity, too. In fact, 2 bar of air are not sufficient to obtain the product (selectivity is zero), while increasing the pressure selectivity increases as well, even if it still does not reach good results. Moreover, the nature of the oxidant has a very noticeable effect on the reaction selectivity: On equal pressure terms, oxygen

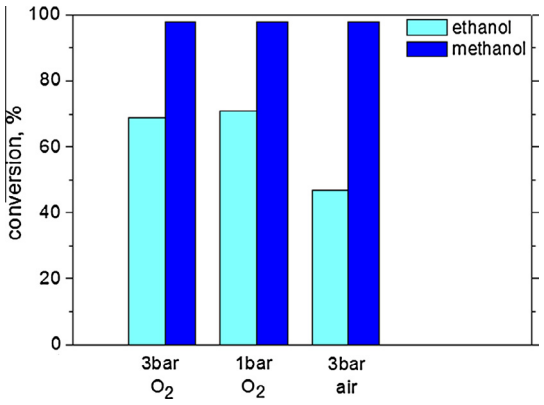

Fig. 10. Furfural oxidative esterification reaction on AuZ catalyst: effect of solvent (120 °C, after 180 min).

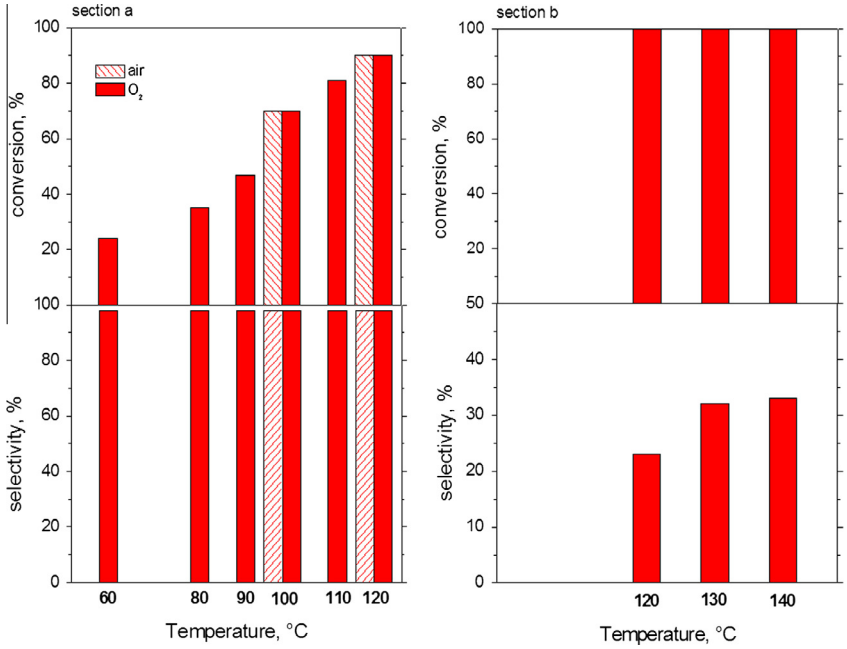

Fig. 11. Effect of the temperature on furfural (section a, autoclave charged with 6 bar of O_2 after 90 min) and HMF (section b, autoclave charged with 3 bar of O_2, after 5 h) oxidative esterification reactions on the AuZ catalyst.

performs 50% better than air. Using molecular oxygen as oxidant, the conversions are always absolute. In addition, no appreciable changes in terms of product selectivity can be noted varying the oxygen from 6 until 1 bar. Therefore, the choice of the oxidant is very important for HMF oxidative esterification: Oxygen is better than air as an oxidant, firstly due to dilution effect. However, some further considerations on the effect of oxygen can be done. HMF molecule can interact with the surface of the catalyst mainly with the aldehydic —C═O group and, differently from furfural, by means of the —OH group as well. We can reasonably assume that, as for intrinsic reactivity, this alcoholic group possesses features similar to those of the —OH belonging to methanol. A role of oxygen atoms bound to gold clusters in extracting the hydrogen atom of such group giving rise to the alcoholate species can be hypothesised for the activation of HMF [31]. Therefore, as for the HMF oxidative esterification, the presence of basic oxygen atoms is required for both methanol and HMF reactants, explaining the enhanced oxygen sensitivity of this reaction if compared to furfural oxidative esterification.

Nevertheless, depending on the industrial needs, it is possible to operate at both low (1 bar) and higher (6 bar) oxygen pressures. In the first chance, there are fewer safety problems and costs for gases, while in the second event, it is possibly to limit the costs by reducing the reactor volume.

3.2.3. Effect of the temperature

The study of the effect of the reaction temperature on the catalytic performances for furfural esterification was performed at 90 min of reaction, with a pressure of 6 bar of oxygen, lowering temperature from 120 °C until 60 °C. The screening, reported in Fig. 11 (section a), highlights a marked temperature effect on the furfural conversion.

More in detail, a decrease in the temperature from 120 to 60 °C causes a 70% drop in the conversion. The same trend is found as for tests conducted in air at a pressure of 3 bar (lines bars). On the contrary, the results obtained for the selectivity are unrelated to the reaction temperature. FTIR experiments (see Fig. 3) demonstrated that the higher is the temperature, the higher is the intensity of the band related to methylfuroate. However, no bands due to other reaction intermediates have been observed neither at RT nor at 120 °C, indicating that direct selective oxidation of furfural to the desired furoate is occurring (see Section 3.1.1). Therefore, the temperature has no effect on the selectivity.

These data, together with the findings on the effect of the pressure, demonstrated that both pressure and temperature are independent from the choice of the oxidant in the investigated ranges. In order to find the best compromise among costs, heating time and conversion, a reaction temperature of 100 °C for furfural esterification can be suggested, allowing only a small improvement for the overall process.

The kinetic behaviour of the AuZ sample in the furfural oxidative esterification was investigated, too. Examples of kinetic curves, referring to different reaction temperatures, are given in Fig. 12.

As previously discussed, an appreciable decrease in specific activity occurs by decreasing the reaction temperature from 120 °C to 60 °C. The reaction order with respect to furfural was found to be one. To check for possible influence of pore diffusion, even if highly improbable, due to the very small particle size used (lower than 0.1 mm), the activation energy was measured for the

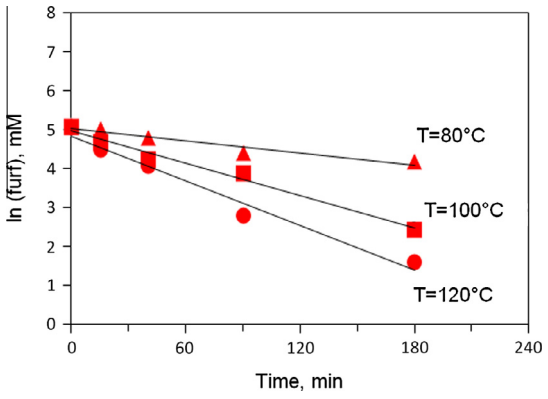

Fig. 12. First order plots for oxidative esterification of furfural on AuZ catalyst at different reaction temperatures. Triangles = 80 °C; squares = 100 °C; circles = 120 °C.

AuZ catalyst. A value of 38.9 kJ/mol was obtained, thus ruling out any appreciable influence of pore diffusion in our kinetic data.

The effect of the reaction temperature on the catalytic performances for HMF oxidative esterification is shown in Fig. 11 (section b). Conversion is always complete under the reported experimental conditions. Moreover, looking at selectivity, there are no substantial differences between 130 °C and 140 °C in terms of FDMC formation. On the contrary, a remarkable effect can be observed if the temperature is decreased from 130 to 120 °C. In such case, the selectivity approximately decreases of 30%. Therefore, no advantages can be achieved by increasing the reaction temperature until 140 °C.

4. Conclusions

The use of heterogeneous catalysis for the exploitation of renewable raw materials such as ligno-cellulosic biomass is allowing the development of a "new chemistry" with enormous potential, addressing processes and products more sustainable for both environment and economic point of view. Good results on the furfural and HMF oxidative esterification reactions have been obtained in the presence of the gold catalyst supported on zirconia, even without the use of a base such as sodium methoxide, which makes the process less sustainable from the environmental and economic point of view. The oxygen molecule is activated on gold and the reaction follows the direct way of the oxidation from the substrate into the desired product. The spectroscopic findings pointed out that both furfural and methylfuroate interact mainly through their carbonylic group with the surface of the catalyst. Moreover, FTIR data confirm that the formation of the product seems to occur without formation of any adsorbed intermediate species and that the reaction proceeds through direct selective oxidation of furfural to the desired furoate.

For both furfural and HMF processes, a considerable effect of the reaction temperature has been evidenced in the range here investigated (60–140 °C). The spectroscopic results indicate that gold on zirconia catalyst is able to catalyse the furfural esterification already at RT, giving an almost complete selectivity to methyl-2-furoate. FTIR data indicate also that reaction temperature has no effect on the selectivity of the reaction.

The optimisation of the reaction time for the furfural oxidative esterification allows making more efficient the batch reactor, since it allows more cycles and smaller size of plant.

Oxygen relative pressure can be lowered from 6 to 1 bar without significant changes in the catalytic performances, leading to a significant increase in the process safety and a decrease in the costs of plant. The replacement of the oxidant by the more economic air, still at very low relative pressure guarantees to operate safely outside the explosion range. Moreover, with a view to a future application of the process on a large scale, there are relevant economic benefits. Along with the catalyst recycling previously verified, these results suggest that the industrial process to oxidised product is feasible, and lead to an efficient and sustainable process.

The study performed on the HMF oxidative esterification at different times of reaction indicated that a complete conversion is reached after 3 h. As regards the air as an oxidant, the pressure increase has strong effects both in terms of conversion and selectivity. On the contrary, as regards oxygen as oxidant, selectivity remains unchanged with pressure. From the comparison of the two oxidants at the same pressure used is apparent that the best choice is to employ oxygen (1 bar).

The spectroscopic results confirm that in reaction conditions, oxygen is fundamental to keep the active surface sites free, in particular the highly dispersed gold sites, where oxygen can be dissociated. As a consequence, the amount of oxygen is a crucial point. In particular, the presence of basic oxygen atoms is required for both methanol and HMF reactants, explaining the enhanced oxygen sensitivity of this reaction if compared to furfural oxidative esterification.

Acknowledgments

We thank Mr. Alvise Vivian and Mr. Damiano Marchese for their work. Financial support to this work by MIUR-Italy (Cofin 2008) is gratefully acknowledged.

Appendix A. Supplementary material

Supplementary data associated with this article can be found, in the online version, at http://dx.doi.org/10.1016/j.jcat.2014.07.017.

References

[1] B. Kamm, P. Gruber, M. Kamm, Biorefineries—Industrial Processes and Products, Status quo and Future Directions, vols. 1 and 2, Wiley-VCH, Weinheim, 2005.
[2] H. Röper, Starch 54 (2002) 89–99.
[3] S. Fernando, S. Adhikari, C. Chandrapal, N. Murali, Energy Fuels 20 (2006) 1727–1737.
[4] X. Tong, Y. Ma, Y. Li, Appl. Catal. A 385 (2010) 1–13. and references therein.
[5] M. Bicker, J. Hirth, H. Vogel, Green Chem. 5 (2003) 280–284.
[6] H. Koslowski, Chem. Fibers Int. 57 (6) (2007) 287–293.
[7] R.J. Sheehan, Ullmann's Encyclopedia of Industrial Chemistry, vol. A26, VCH Verlags, Weinheim, 1995. p. 193.
[8] F. Menegazzo, T. Fantinel, M. Signoretto, F. Pinna, Catal. Commun. 8 (2007) 876–879.
[9] T. Werpy, G. Petersen, Report No. NREL/TP-510-35523, 2004.
[10] E. Taarning, I.S. Nielsen, K. Egeblad, R. Madsen, C.H. Christensen, ChemSusChem 1 (2008) 75–78.
[11] O. Casanova, S. Iborra, A. Corma, J. Catal. 265 (2009) 109–116.
[12] www.avantium.com/yxy.
[13] F. Pinna, A. Olivo, V. Trevisan, F. Menegazzo, M. Signoretto, M. Manzoli, F. Boccuzzi, Catal. Today 203 (2013) 196–201.
[14] M. Signoretto, F. Menegazzo, L. Contessotto, F. Pinna, M. Manzoli, F. Boccuzzi, Appl. Catal. B 129 (2013) 287–293.
[15] F. Menegazzo, M. Signoretto, F. Pinna, M. Manzoli, V. Aina, G. Cerrato, F. Boccuzzi, J. Catal. 309 (2014) 241–247.
[16] S.E. Davis, M.S. Ide, R.J. Davis, Green Chem. 15 (2013) 17–45.
[17] X. Tong, Y. Ma, Y. Li, Appl. Catal. A 385 (2010) 1–13.
[18] A. Rosatella, S.P. Simeonov, R.F.M. Frade, C.A.M. Afonso, Green Chem. 13 (2011) 754–793.
[19] F. Menegazzo, F. Pinna, M. Signoretto, V. Trevisan, F. Boccuzzi, A. Chiorino, M. Manzoli, ChemSusChem 1 (2008) 320–326.
[20] F. Menegazzo, F. Pinna, M. Signoretto, V. Trevisan, F. Boccuzzi, A. Chiorino, M. Manzoli, Appl. Catal. A 356 (2009) 31–35.
[21] C. Morterra, G. Cerrato, V. Bolis, S. Di Ciero, M. Signoretto, J. Chem. Soc. Faraday Trans. 93 (1997) 1179–1184.
[22] M. Bensitel, O. Saur, J-C. Lavalley, G. Mabilon, Mater. Chem. Phys. 17 (1987) 249–258.
[23] C. Morterra, V. Bolis, B. Fubini, L. Orio, Surf. Sci. 251 (252) (1991) 540–545.
[24] G. Martra, Appl. Catal. A: Gen. 200 (2000) 275–283.
[25] F. Boccuzzi, A. Chiorino, M. Manzoli, P. Lu, T. Akita, S. Ichikawa, M. Haruta, J. Catal. 202 (2001) 256–257.
[26] F. Boccuzzi, A. Chiorino, M. Manzoli, J. Power Sources 118 (2003) 304–310.
[27] M. Manzoli, A. Chiorino, F. Boccuzzi, Appl. Catal. B 57 (2005) 201–209.
[28] T. Baker, X. Liu, C.M. Friend, Phys. Chem. Chem. Phys. 13 (2011) 34–46.
[29] B. Xu, X. Liu, J. Haubrich, C.M. Friend, Nat. Chem. 2 (2010) 61–65.
[30] B. Lewis, G. von Elbe, Combustion, Flames and Explosion of Gases, Academic Press, New York, 1961.
[31] X. Liu, C. Friend, Langmuir 26 (2010) 16552–16557.